Electronic Supplementary Material (ESI) for Physical Chemistry Chemical Physics.

Electronic Supplementary Information (ESI)

Morphology control of zinc electrodeposition by surfactant addition for alkaline-based rechargeable batteries

[a] Department of Materials Chemistry, Faculty of Engineering, Shinshu University
[b] Institute of Carbon Science and Technology, Faculty of Engineering, Shinshu University
4-17-1 Wakasato, Nagano 380-8553, Japan

Masahiro Shimizu*[ab], Koichi Hirahara[a], Susumu Arai*[ab]

Dr. Masahiro Shimizu
E-mail: shimizu@shinshu-u.ac.jp
Tel: +81-26-269-5627; Fax: +81-26-269-5627

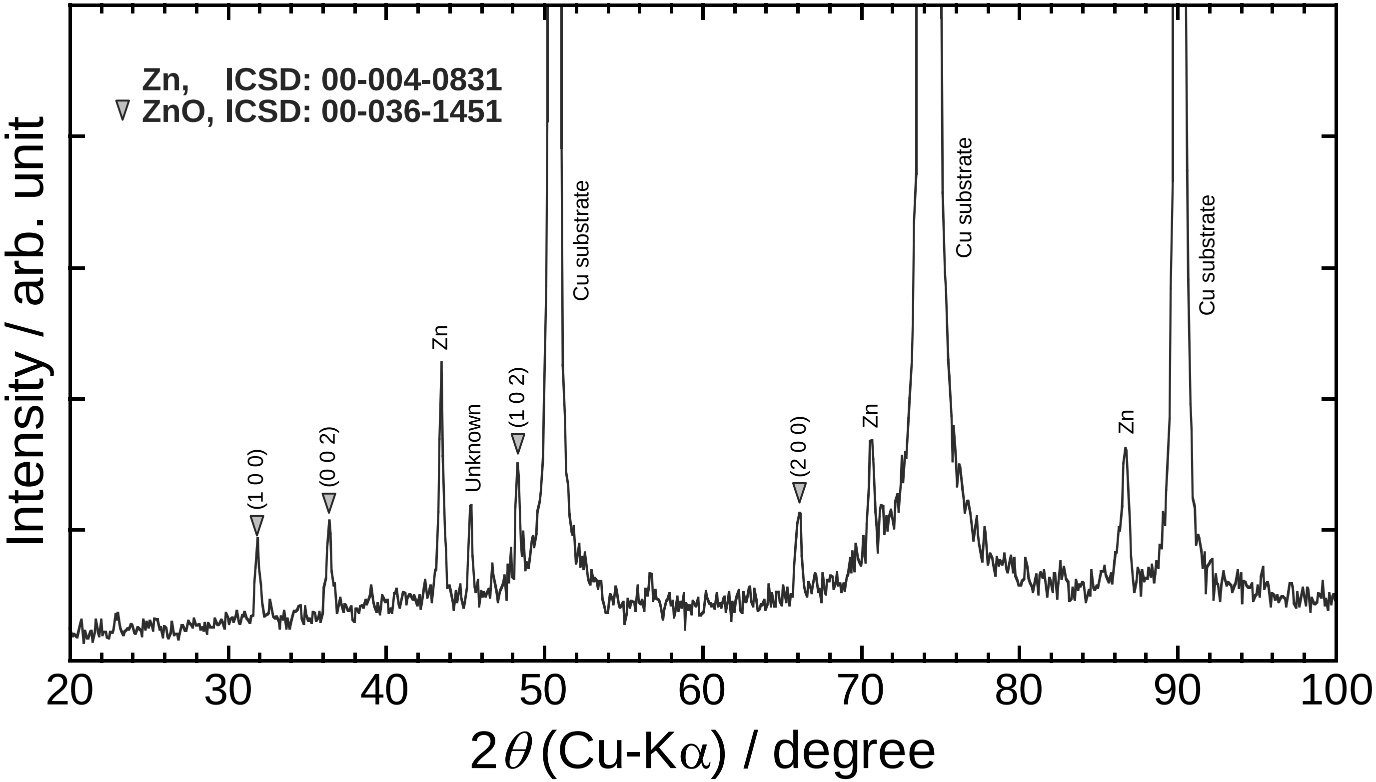

Figure S1. XRD pattern of a Cu substrate at the potential of 0.2 V vs. Zn/Zn^{2+} in an additive free electrolyte. The cyclic voltammetry was stopped when sweeping to positive potential and the XRD measurement was conducted. Peaks associated with the formation of ZnO was confirmed, which indicates that the second oxidation peak is attributed to the formation of such passivation layer.

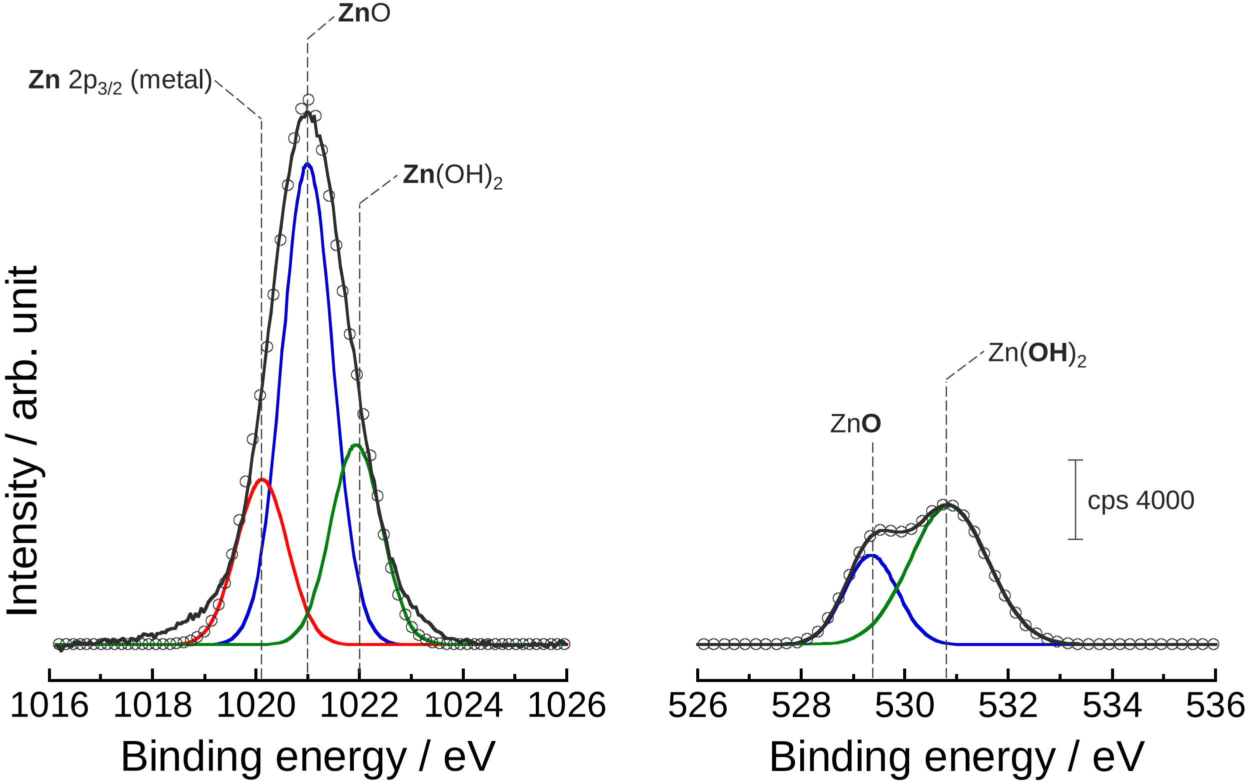

Figure S2. XPS spectra of (a) Zn 2p and (b) O 1s regions of Zn deposit obtained from a zincate solution (additive free). The spectra (recorded before Ar-etching) were deconvoluted into several components using a Gauss function. In the Zn 2p and O 1s regions, the black, circle, red, blue, green lines correspond to the observed spectrum, the total spectrum, and the deconvoluted components of Zn metal, ZnO, and $Zn(OH)_2$.

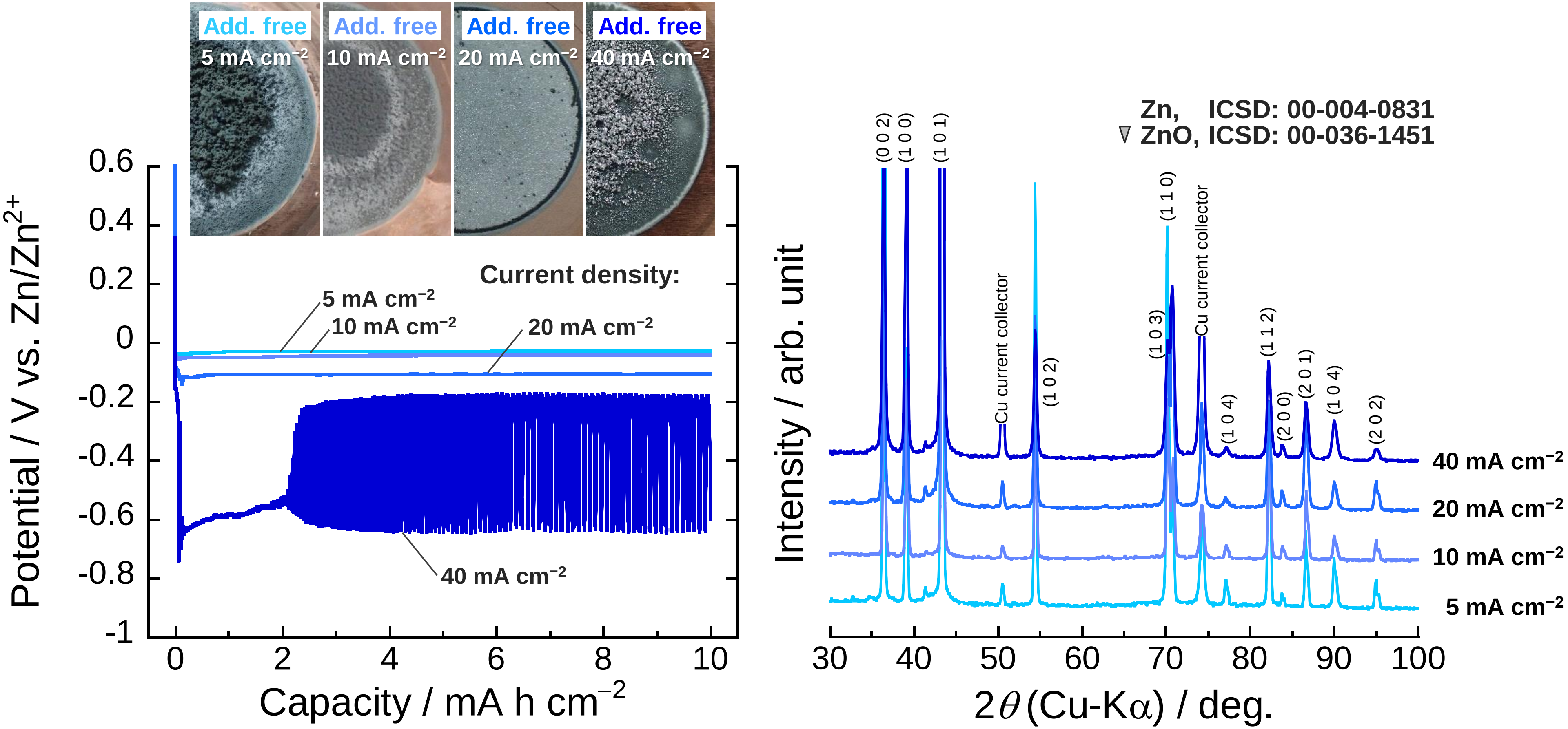

Figure S3. Electrochemical Zn deposition behaviors in an aqueous solution of 0.25 M ZnO + 4 M KOH (additive free) under various current densities. The overpotential against equilibrium potential ($Zn^{2+} + 2e^{-} \rightarrow Zn$) in the respective condition was 28 mV (5 mA cm^{-2}), 40 mV (10 mA cm^{-2}), 107 mV (20 mA cm^{-2}).

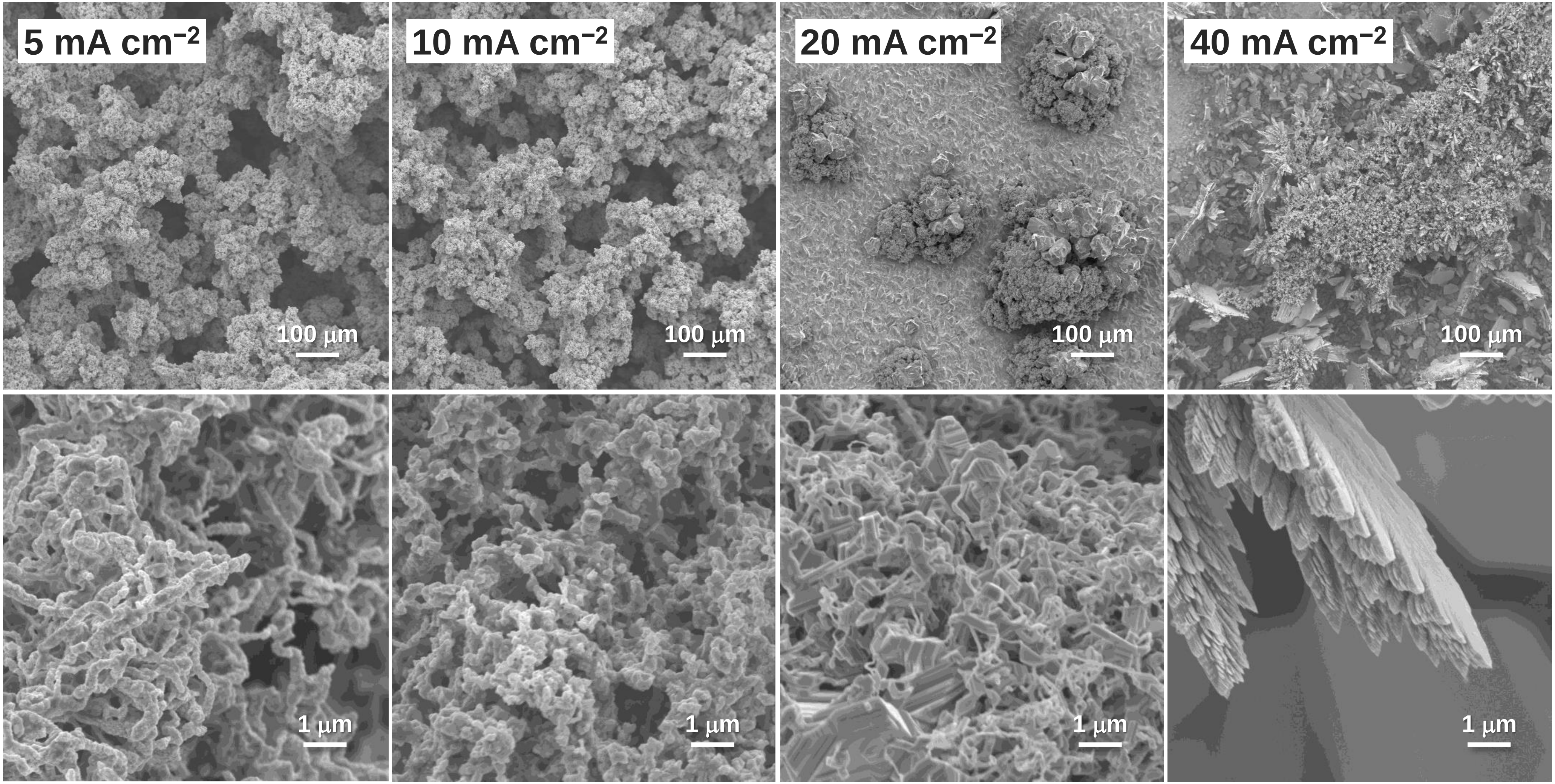

Figure S4. FE-SEM images of electrochemically grown Zn on a Cu substrate in a **surfactant-free** aqueous solution of 0.25 M ZnO/4 M KOH under various current densities. Charge capacity is 10 mA h cm^{-2}.

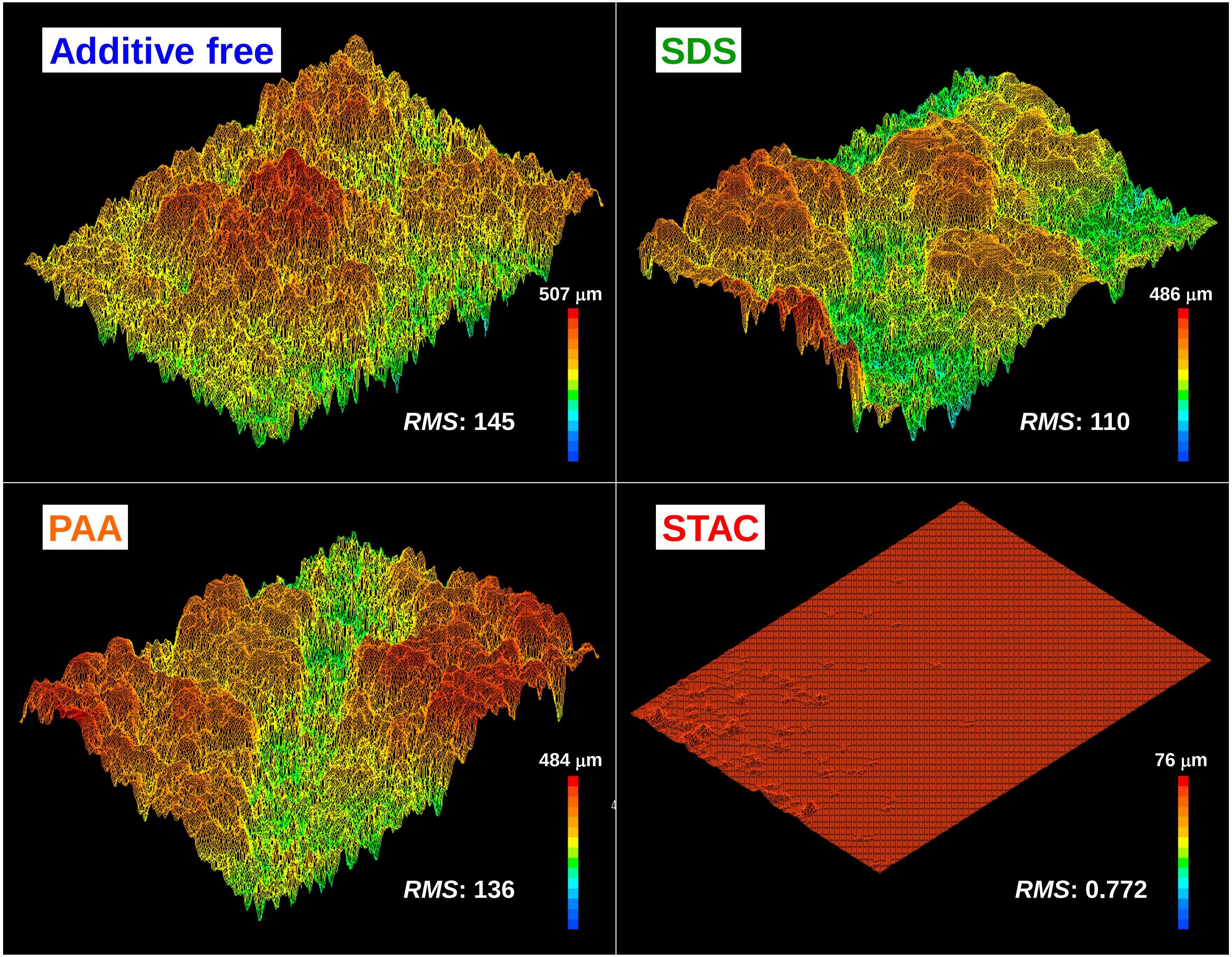

Figure S5. Three-dimensional height profiles of Zn morphologies deposited form various electrolyte with 1 mM surfactant (additive free, SDS, PAA, and STAC).

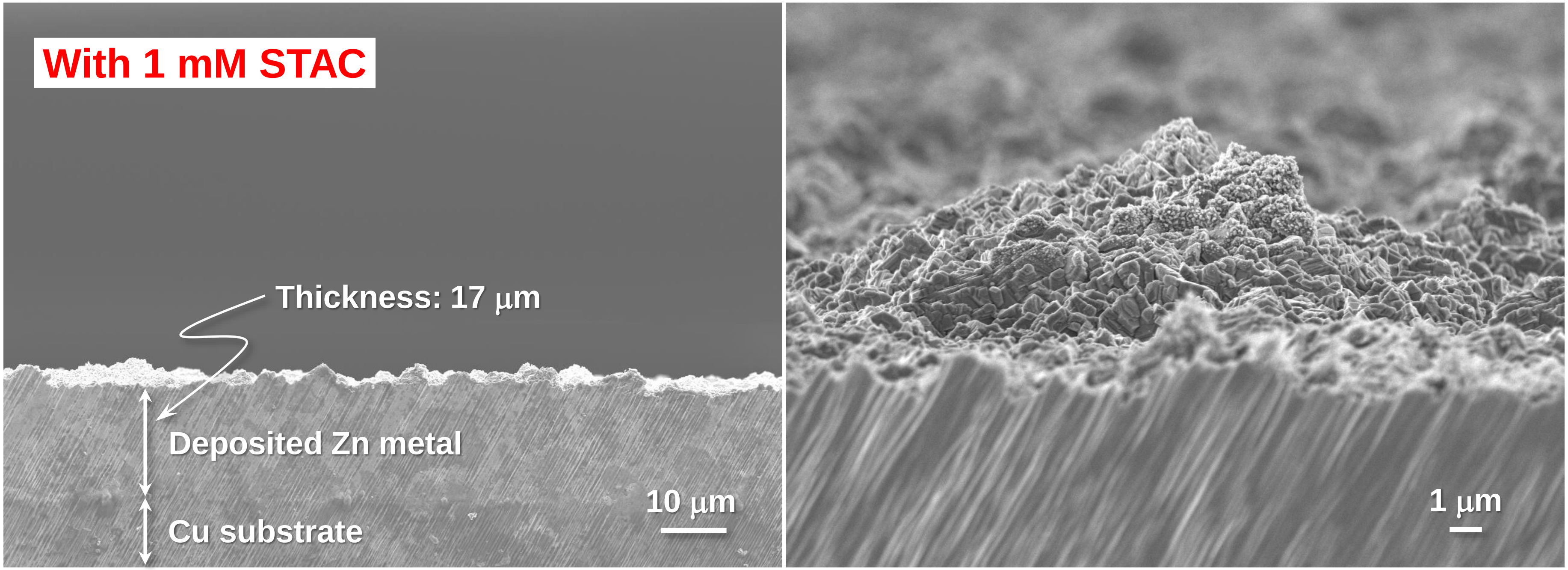

Figure S6. Cross-sectional FE-SEM images and enlarged views of Zn deposits obtained from an electrolyte solution containing 1 mM STAC. The charge capacity corresponding to Zn deposition is 10 mA h cm^{-2}. Because the area of working electrode (Cu current collector) was set to 1.7 cm^2, the theoretical thickness of Zn deposit is 17 μm. It is noteworthy that the obtained thickness is good agreement with the theoretical one, which indicates that STAC surfactant with cationic charge acts as a leveling agent during Zn deposition.

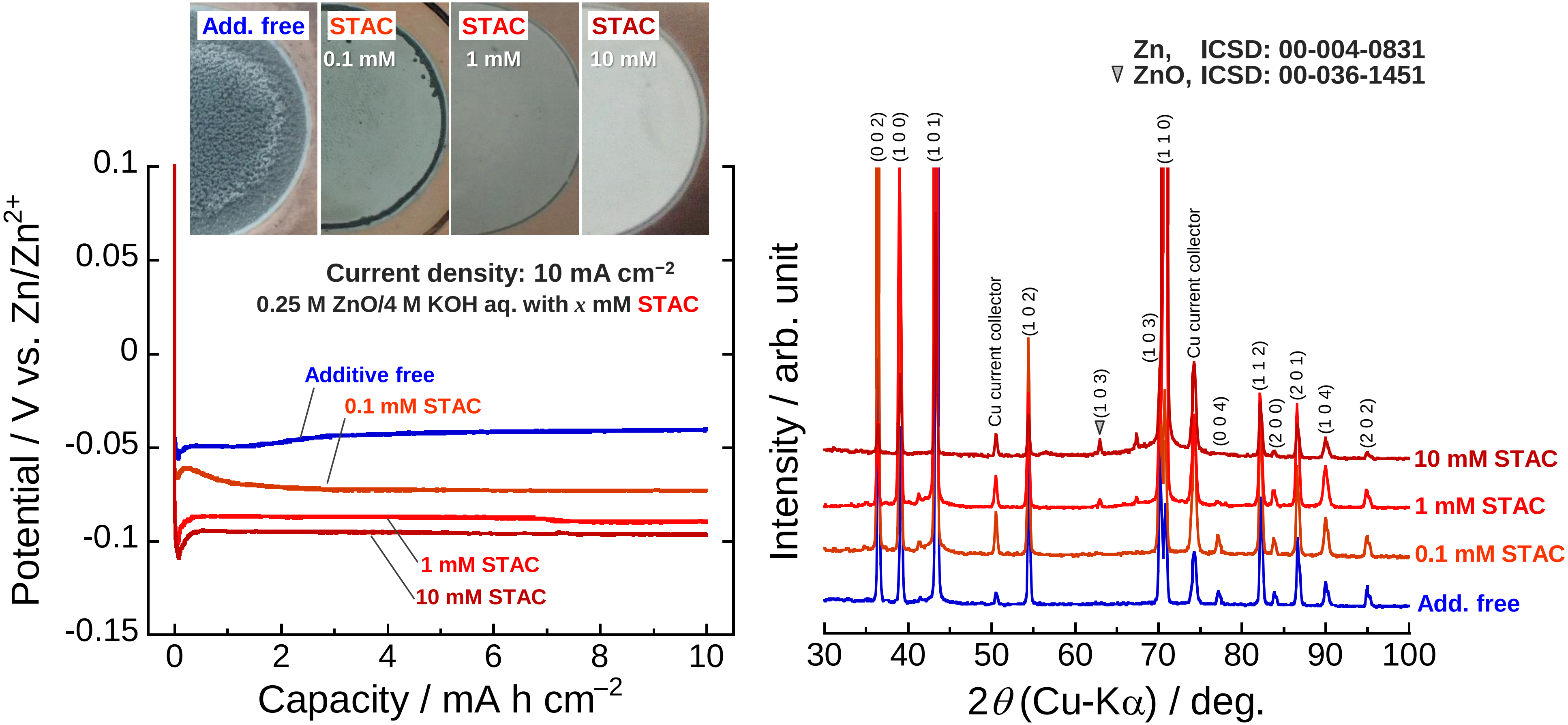

Figure S7. (a) STAC concentration dependence on charge (Zn deposition) behavior in zincate solution. Current density was set to 10 mA cm^{-2}. (b) XRD patterns of the deposits obtained from the electrolytes. The overpotential against equilibrium potential ($Zn^{2+} + 2e^{-} \rightarrow Zn$) in the respective electrolyte was 40 mV (additive free), 70 mV (0.1 mM STAC), 90 mV (1 mM), and 97 mV (10 mM).

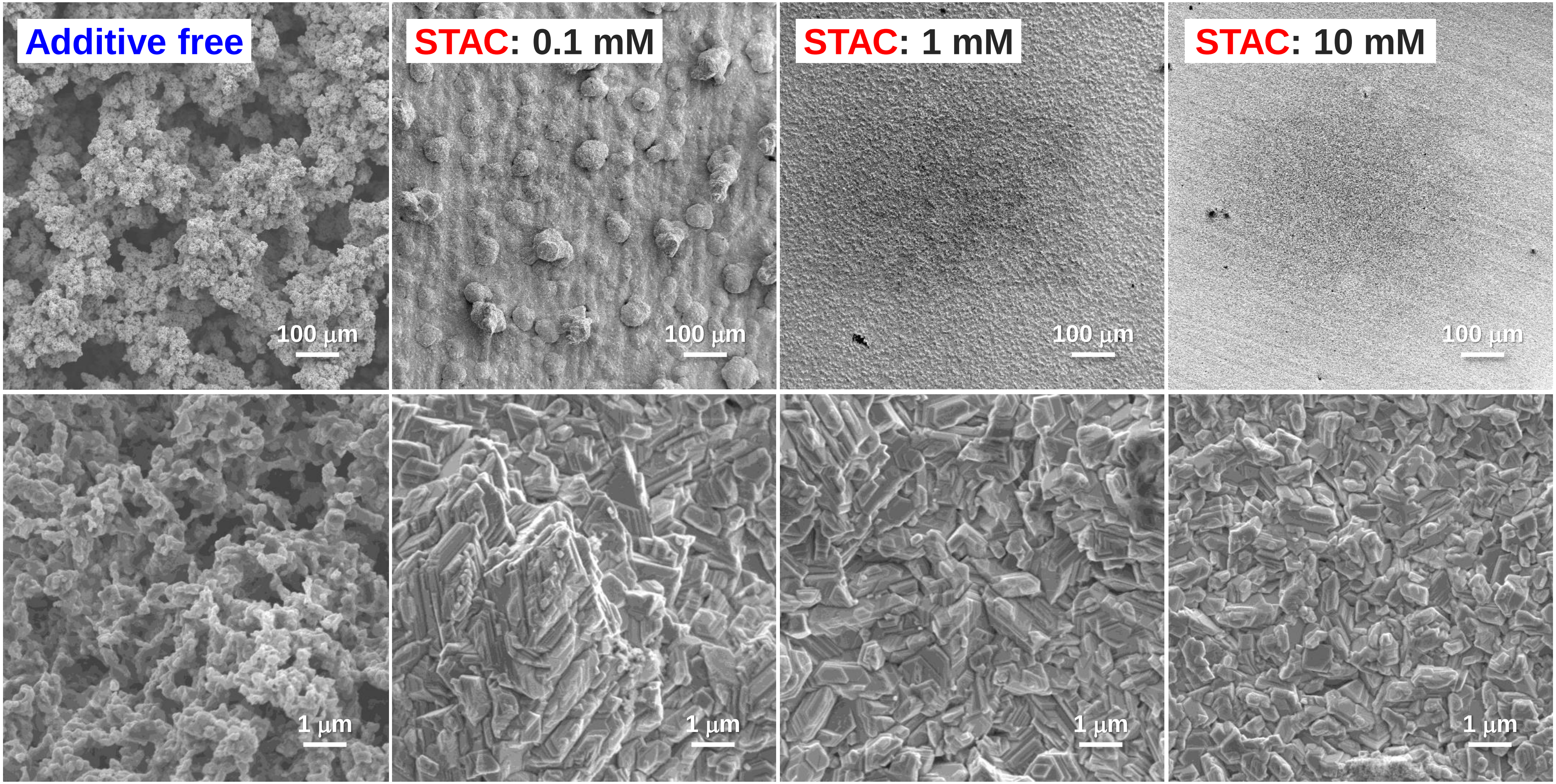

Figure S8. Influence of STAC concentration on Zn deposition morphology in an aqueous solution of 0.25 M ZnO/4 M KOH. FE-SEM images of Zn deposited at current density of 10 mA h cm^{-2}. Magnification: 100 (top), 10000 (bottom).

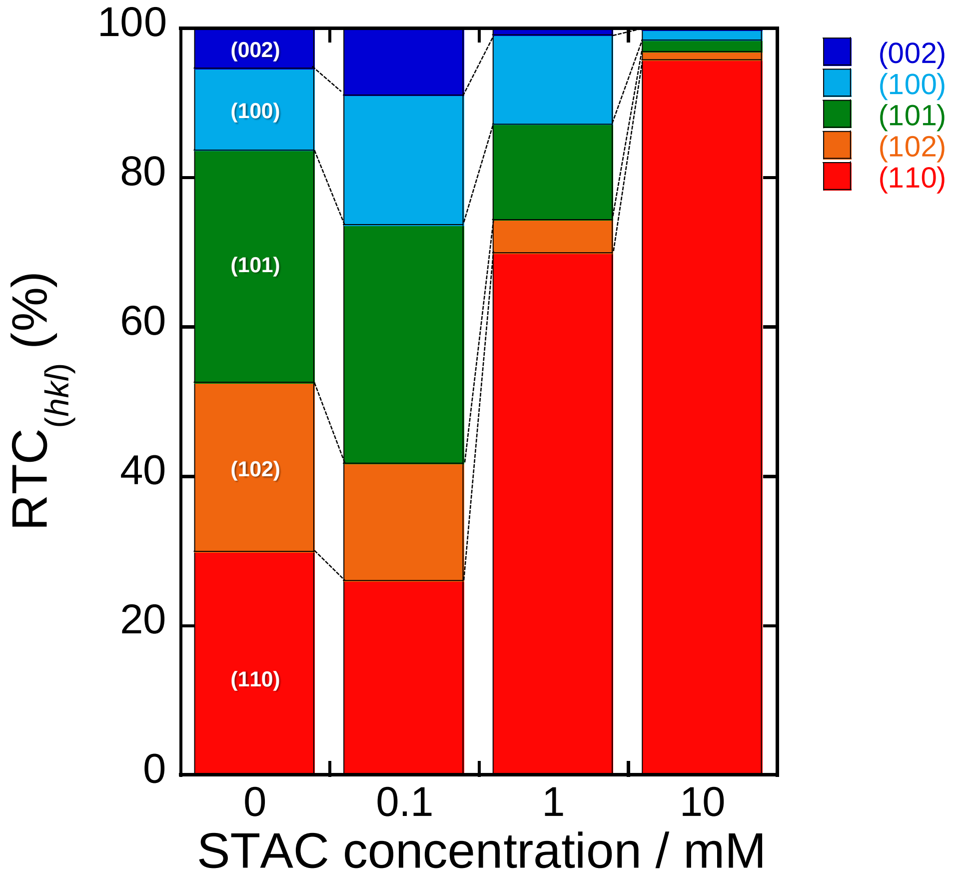

Figure S9. Variation in the relative texture coefficient for Zn (110), (002), (100), (101), and (102) diffraction peaks as a function of charge capacity in 0.25 M ZnO/4M KOH with *x* mM STAC (*x*=0, 0.1, 1, 10). As a reference, commercially available Zn powder that is randomly orientated was used.

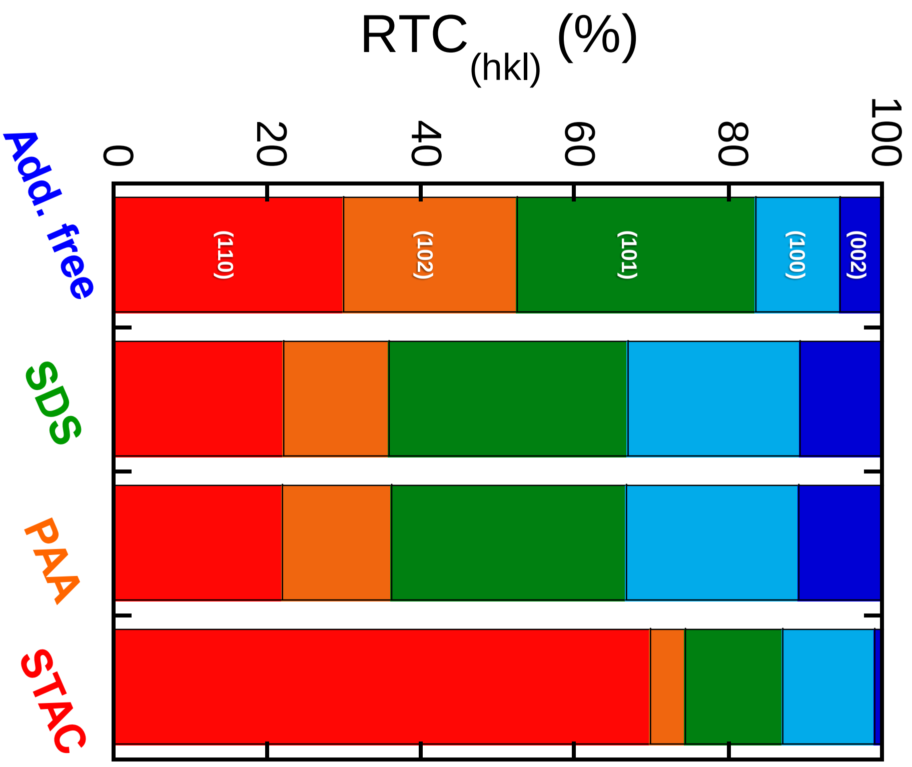

Figure S10. Relative texture coefficient for Zn (110), (002), (100), (101), and (102) diffraction peaks in electrolyte solutions (0.25 M ZnO/4M KOH) without and with 1 mM additive. Zn deposit was electrochemically grown for capacity of 10 mA h cm^{-2} under constant current density of 10 mA cm^{-2}. It is clear that there is no significant difference in orientation for Zn deposits obtained from an additive free electrolyte and electrolytes with 1 mM SDS or PAA.

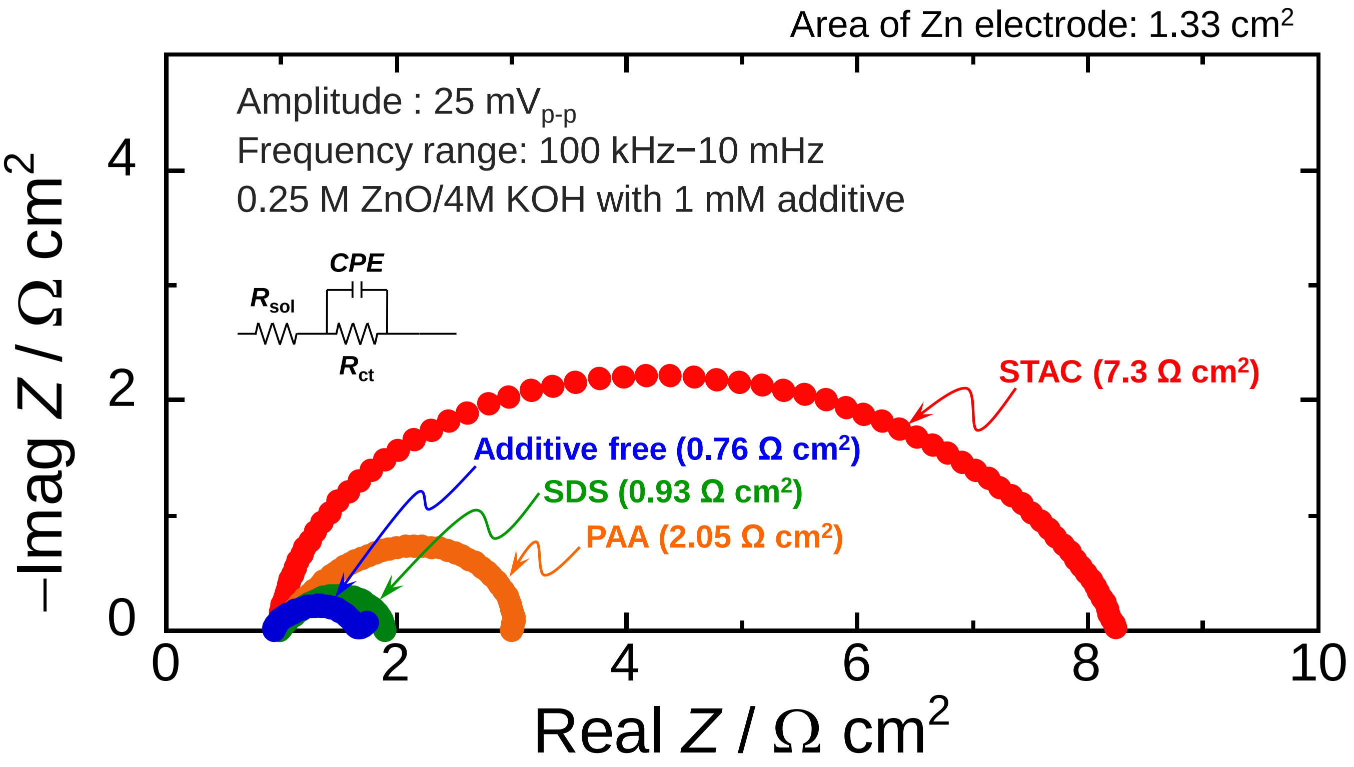

Figure S11. Nyquist plots of symmetric Zn|Zn metal sheets cells in 0.25 M ZnO/4 M KOH with 1 mM additive at 303 K. Inset: the equivalent circuit for impedance analysis. SDS with a negative charge does not involve in charge transfer reaction associated with Zn-deposition/dissolution and the resistance value depending the size of a semicircle is same degree in comparison with that in an additive free electrolyte. Although PAA has an influence on charge transfer, the resistance far smaller than that in 1 mM-SATC containing electrolyte. Thus, we consider that cationic surfactant plays a key role of leveling for Zn deposit.

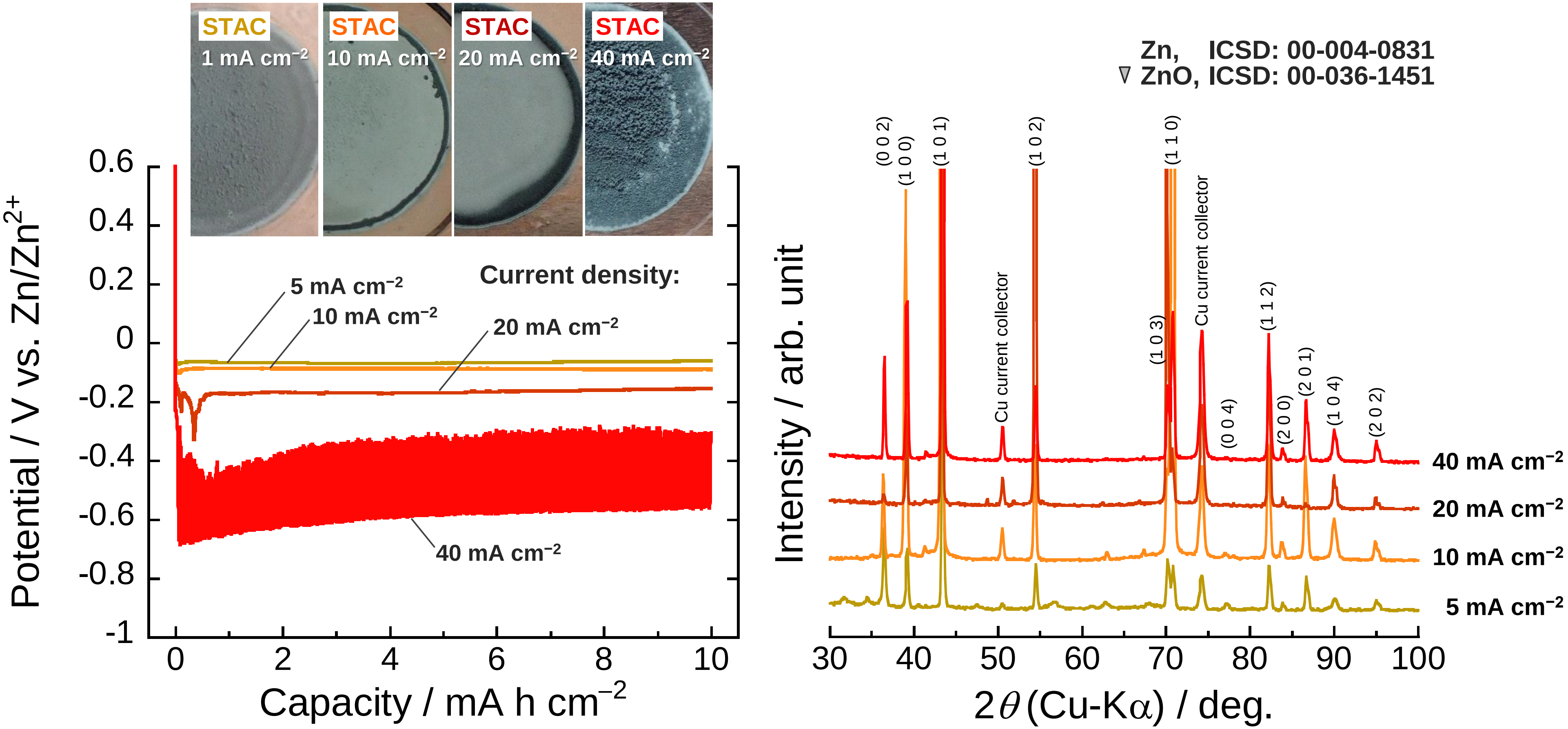

Figure S12. Electrochemical Zn deposition behaviors in an aqueous solution of 0.25 M ZnO + 4 M KOH (additive free) with 1 mM STAC under various current densities. The overpotential against equilibrium potential ($Zn^{2+} + 2e^- \rightarrow Zn$) in the respective condition was 63 mV (5 mA cm^{-2}), 90 mV (10 mA cm^{-2}), 157 mV (20 mA cm^{-2}).

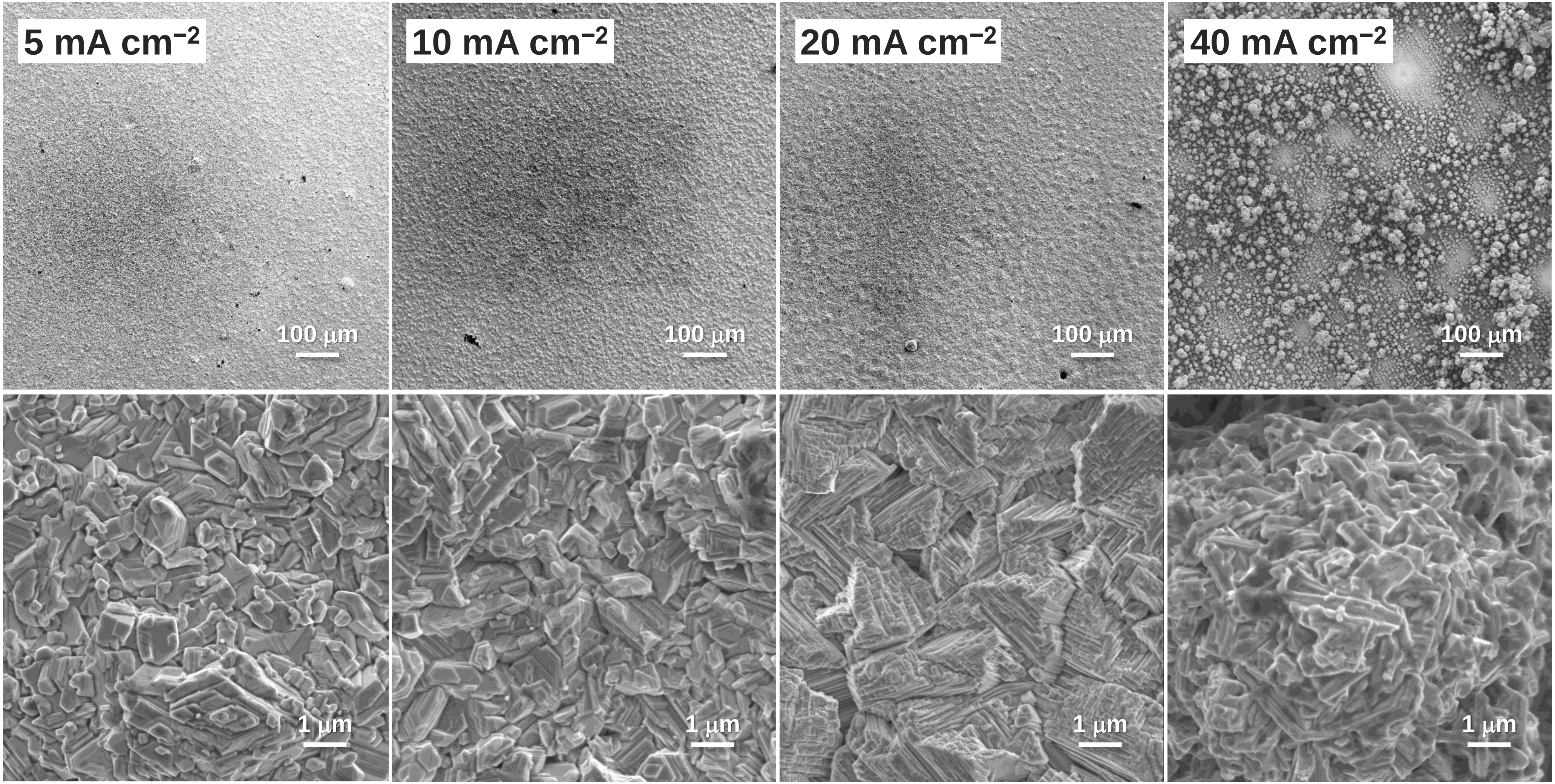

Figure S13. FE-SEM images of electrochemically grown Zn on a Cu substrate in an aqueous solution of 0.25 M ZnO/4 M KOH with 1 mM STAC under various current densities. Charge capacity is 10 mA h cm^{-2}.

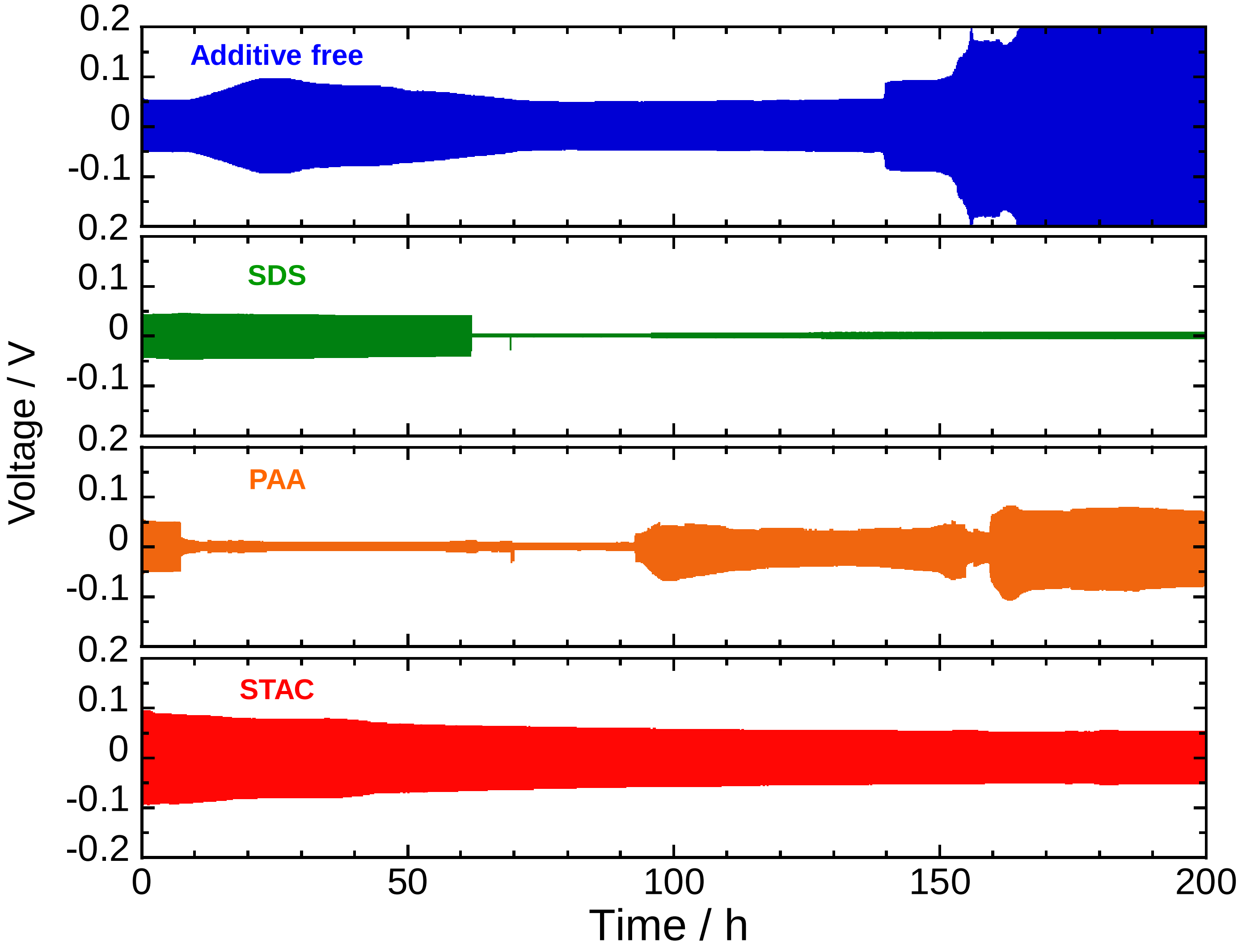

Figure S14. Long-term cycling of symmetric Zn|Zn cells operated under a current density of 10 mA cm^{-2}. The charge/discharge capacities were set to 1 mA h cm^{-2}. The important point to emphasize is that the dependence in 1 mM-containing STAC electrolyte was excellent in reproducibility.

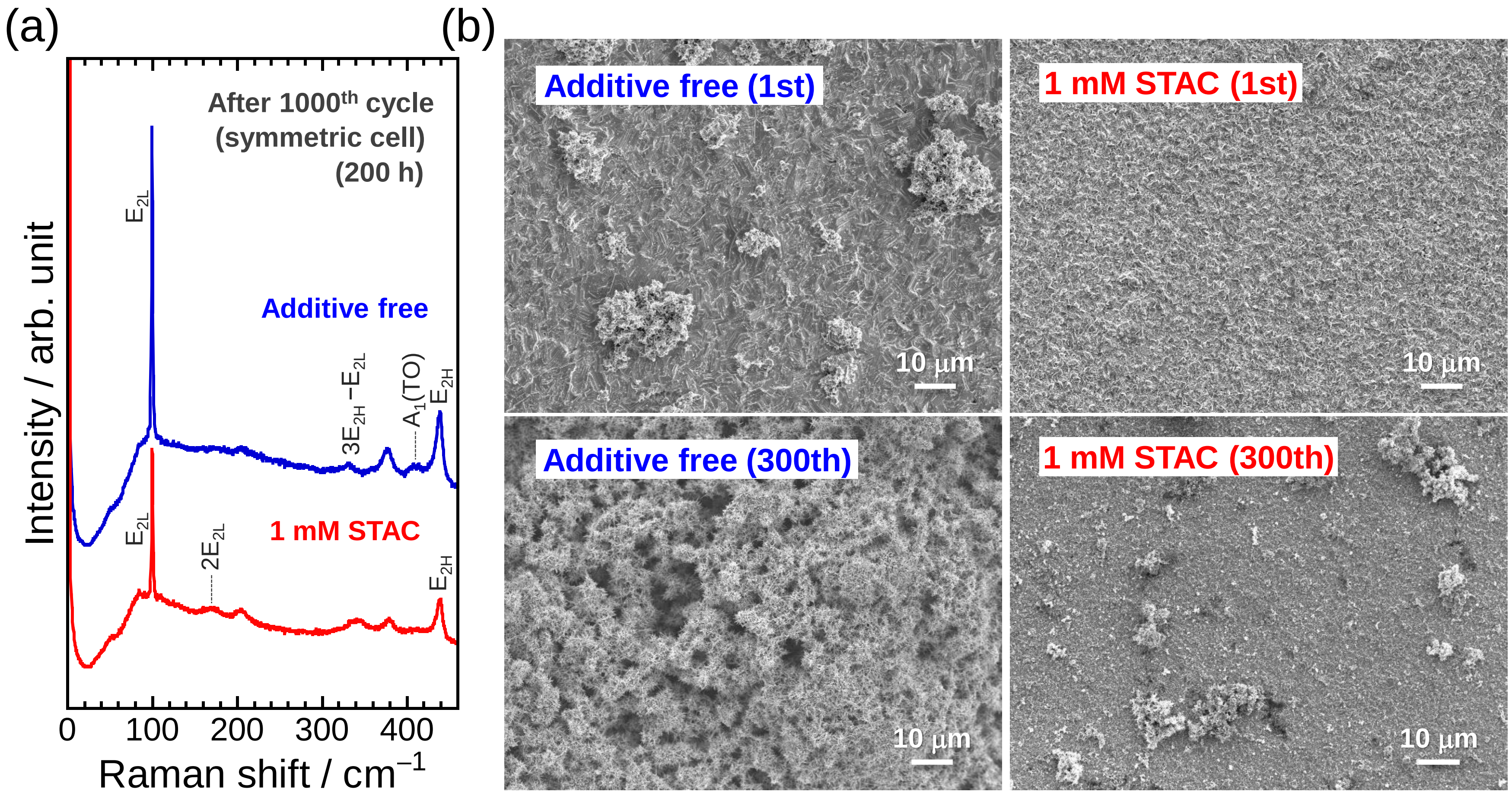

Figure S15. (a) Raman spectra of Zn metal sheets after 1000th (200 h) cycling in electrolyte solutions with and without 1 mM STAC. (b) FE-SEM images of electrochemically grown Zn on a Cu substrate after Zn deposition/stripping. Charge (Zn deposition) capacity and current density are 1 mA h cm^{-2} and 10 mA cm^{-2}, respectively.

Although the formation of ZnO was recognized regardless of the presence or absence of the additive, the band intensity associated with ZnO (100 cm^{-1} / E_{2L}, 165 cm^{-1} / $2E_{2L}$, 300 cm^{-1} / $3E_{2H}–E_{2L}$, 417 cm^{-1} / A_1(TO), and 438 cm^{-1} / E_{2H}) in the 1 mM-STAC containing electrolyte was weaker than that in the additive free electrolyte, which clearly showed that the addition of STAC effectively suppressed surface passivation of Zn metal. We therefore concluded that the sudden increase in overpotential at 156 h in an additive free electrolyte comes from the surface passivation by the accumulation of insulated ZnO on Zn metal surface.

FE-SEM images of Zn grown on a Cu substrate after the first and 300th cycle in the respective electrolytes is displayed in Figure S15b. In the case of absence of any additive, Zn grew in mixture morphologies consisted of flat and mossy structures even under a relatively low Zn deposition capacity of 1 mA h cm^{-2} at the first cycle. In contrast, the addition of 1 mM STAC delivered smooth Zn morphology without mossy structure. After 300th cycling, Zn deposits in the additive free electrolyte underwent a significant change in morphology: no flat-structured Zn was observed.

Reference

1) M. Wang, L. Jiang, E. J. Kim, S. H. Hahn, *RSC Adv.*, **5** (2015) 87496–87503.